8. Miscellaneous

8.1. Grids

As shown by Homework #3, it can be to our advantage to use staggered grid in space

Arakawa and Lamb (1977) compared among others (Winninghoff, (1968); Schoenstadt (1978)) five different arrangements of the dependent variables for dispersion and geostrophic adjustment properties on a square grid.

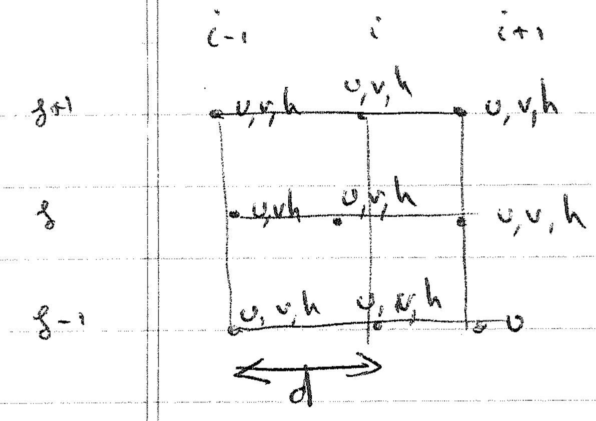

Grid A

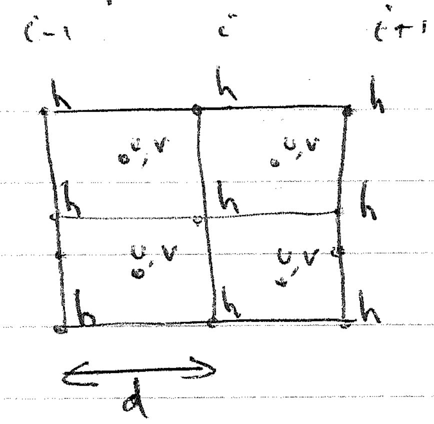

Grid B

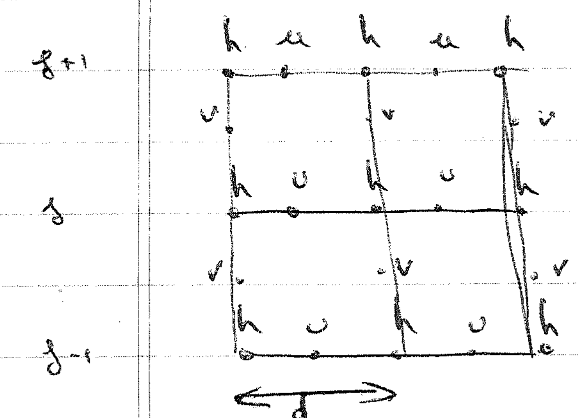

Grid C

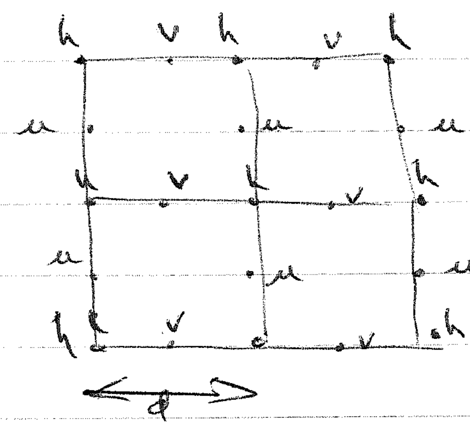

Grid D

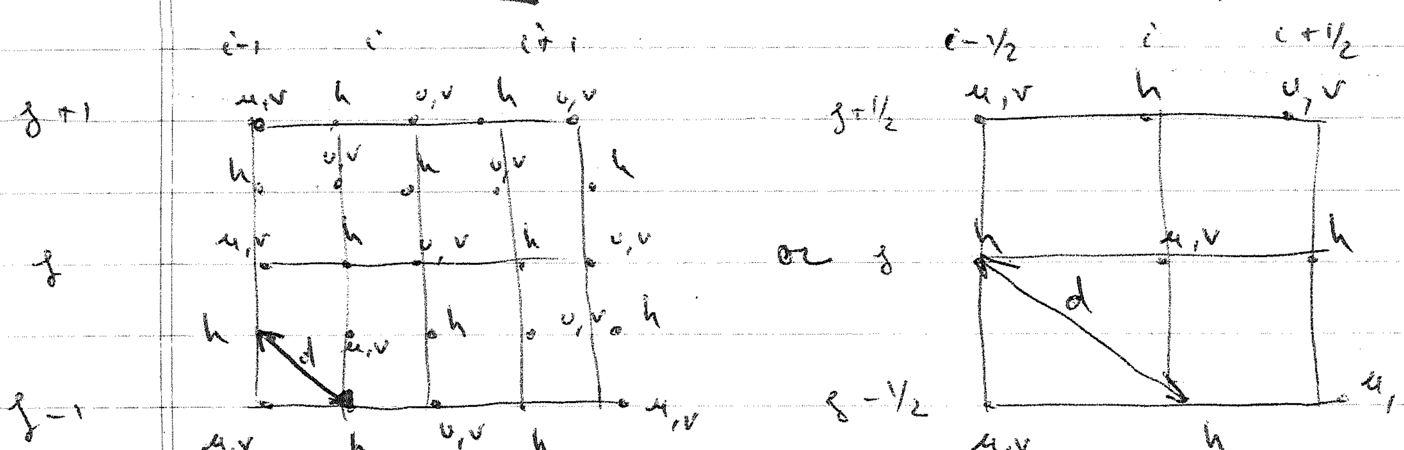

Grid E

②

We now, for purpose of the comparison, redefine the δ and $\overline{(\;)}$

$$\begin{cases} (\delta_x \alpha)_{i,j} = \alpha_{i+1/2,j} - \alpha_{i-1/2,j} \\ (\overline{\alpha}^x)_{i,j} = 1/2\,(\alpha_{i+1} \end{cases}$$

Same for the y direction

For the shallow water equations, we can rewrite the basic linear equations as

<u>Grid A</u>:

$$\frac{\partial u}{\partial t} - fv + g/d\,\overline{(\delta_x h)}^x = 0$$

$$\frac{\partial v}{\partial t} + fu + (g/d)\,\overline{(\delta_y h)}^y = 0$$

$$\frac{\partial h}{\partial t} + \left(H/d\right)\left[\overline{(\delta_x u)}^x + \overline{(\delta_y v)}^y\right] = 0$$

<u>Grid B</u>:

$$\frac{\partial u}{\partial t} - fv + (g/d)\,\overline{(\delta_x h)}^y = 0$$

$$\frac{\partial v}{\partial t} + fu + (g/d)\,\overline{(\delta_y h)}^x = 0$$

$$\frac{\partial h}{\partial t} + \left(H/d\right)\left(\overline{(\delta_x u)}^y + \overline{(\delta_y v)}^x\right) = 0$$

<u>Grid C</u>:

$$\frac{\partial u}{\partial t} - f\overline{v}^{xy} + (g/d)(\delta_x h) = 0$$

$$\frac{\partial v}{\partial t} + f\,\overline{u}^{xy} + (g/d)(\delta_y h) = 0$$

$$\frac{\partial h}{\partial t} + (H/d)\left((\delta_x u) + (\delta_y v)\right) = 0$$

Grid D

$$\frac{\partial u}{\partial t} - f\,\overline{v}^{xy} + (g/d)\,\overline{(\delta_x h)}^{xy} = 0$$

$$\frac{\partial v}{\partial t} + f\,\overline{u}^{xy} + (g/d)\,\overline{(\delta_y h)}^{xy} = 0$$

$$\frac{\partial h}{\partial t} + (H/d)\left(\overline{(\delta_x u)}^{xy} + \overline{(\delta_y v)}^{xy}\right) = 0$$

Grid E

$$\frac{\partial u}{\partial t} - fv + \left(g/d^*\right)(\delta_x h) = 0$$

$$\frac{\partial v}{\partial t} + fu + \left(g/d^*\right)(\delta_y h) = 0$$

$$\frac{\partial h}{\partial t} + \left(\frac{H}{d^*}\right)\left((\delta_x u) + (\delta_y v)\right) = 0$$

In the latter (Grid E), a grid distance of $\sqrt{2}d = d^*$ gives the same number of grid points as the other schemes given a two-dimensional domain.

In order to illustrate the properties of these 5 schemes, we consider the one dimensional linear equations

$$\begin{cases} \dfrac{\partial u}{\partial t} - fv + g\left(\dfrac{\partial h}{\partial x}\right) = 0 \\ \dfrac{\partial v}{\partial t} + fu = 0 \\ \dfrac{\partial h}{\partial t} + H\left(\dfrac{\partial u}{\partial x}\right) = 0 \end{cases}$$

Eliminating v, h yields to

(1) $$\frac{\partial^2 u}{\partial t^2} + f^2 u - gH\left(\partial^2 u/\partial x^2\right) = 0$$

If we assume the solution to be

proportional to $e^{i(kx - \omega t)}$, then the angular frequency ω is given by

(2) $$(\omega/f)^2 = 1 + gH\left(\frac{k}{f}\right)^2 = 1 + k^2 \underline{Rd}^2$$

(Inertia - Gravity waves)

External Rossby Radius of Deformation $\frac{\sqrt{gH}}{f}$

We can now examine the effect of the space discretization on the frequency. In one dimension, the grids become

Grid A:

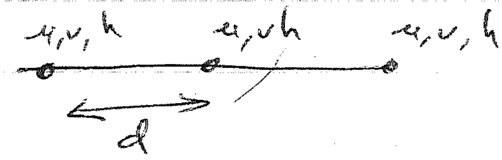

Grid B:

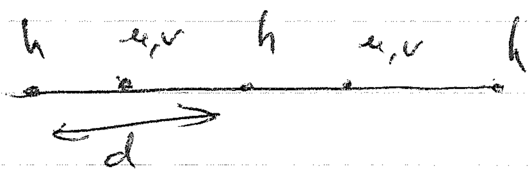

Grid C:

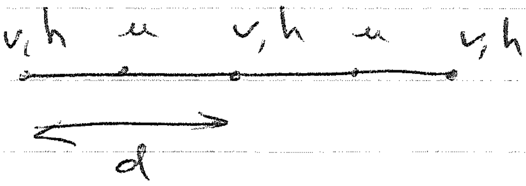

Grid D:

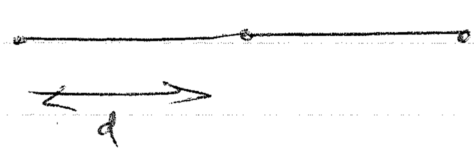

Grid E is equivalent to A, but with a smaller grid size. For the different schemes the following frequencies are obtained (Arakawa and Lamb, 1977)

Grid A: $(\omega/f)^2 = 1 + \left(\frac{Rd}{d}\right)^2 \sin^2 kd$

Grid B: $(\omega/f)^2 = 1 + 4\left(\frac{Rd}{d}\right)^2 \sin^2\left(\frac{kd}{2}\right)$

Grid C: $(\omega/f)^2 = \cos^2\left(\frac{kd}{2}\right) + 4\left(\frac{Rd}{d}\right)^2 \sin^2\left(\frac{kd}{2}\right)$

Grid D: $\left(\frac{\omega}{f}\right)^2 = \cos^2\left(\frac{kd}{2}\right) + \left(\frac{R_d}{d}\right)^2 \sin^2(kd)$

For all cases, ω/f depends on kd and R_d/d
The wavelength of the shortest resolvable wave is $2d$ (corresponding wave number $k_{max} = \pi/d$)
We therefore examine the range $0 < kd < \pi$

Grid A: Maximum for $kd = \pi/2$ with a zero group velocity $\frac{\partial\omega}{\partial k}$

Grid B: For non zero R_d, monotonically increasing

Grid C: Monotonically increasing for $R_d/d > 1/2$ and ________ decreasing for $R_d/d < 1/2$
For $R_d/d = 1/2$ $\omega^2 = f^2$ and the group velocity is zero for all k

Grid D: ω reaches a maximum for $(R_d/d^2) \cos(kd) = 1/4$
$kd = \pi$ is a stationary wave.

For this one dimensional case, grid B is the most satisfactory. However for R_d/d larger than $1/2$, grid C is as good as B

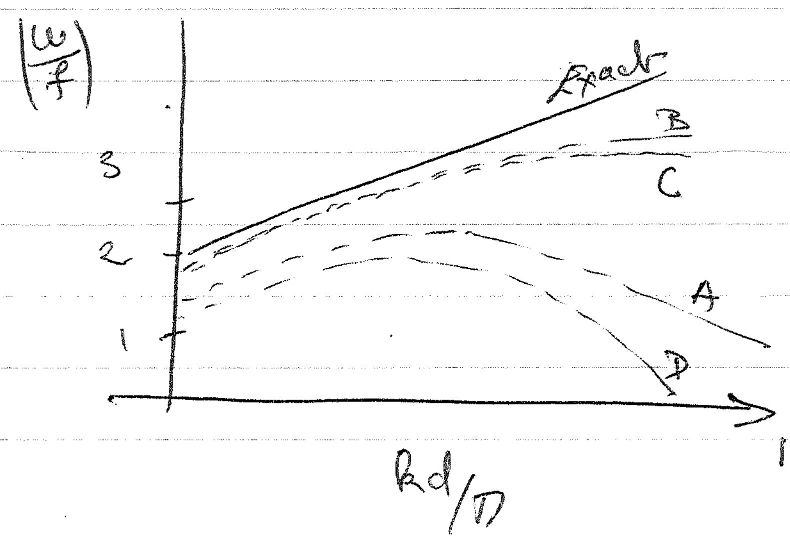

$\boxed{R_d/d = 2}$

As shown in the homework, staggered grids require half the time step that is required for unstaggered grids. However, the extra computer time is worth it with B and C since they give better structure for the shorter waves important after a geostrophic adjustment.

In the two dimensional case, there is a difficulty with B as shown by Arakawa and Lamb (1977)

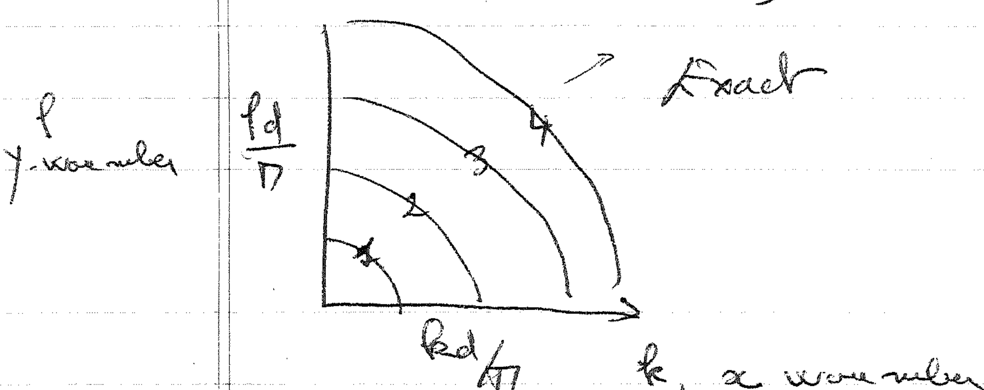

Contours of ω/f

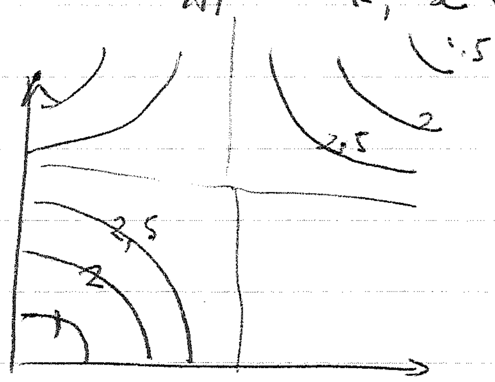

Grid B

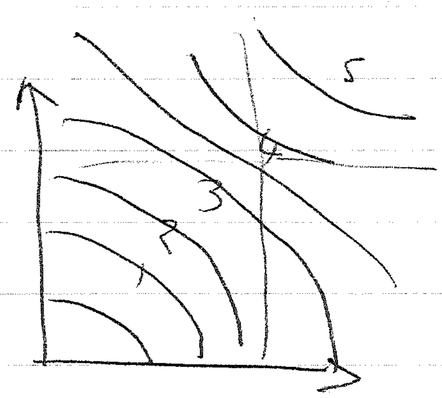

Grid C

For $\frac{R_d}{d} > 1$, Grid C better

$\frac{R_d}{d} < 1$, Grid B better

* The grids can also be staggered in time as proposed by Eliassen (1956) for a baroclinic PE model. Has excellent adjustment properties.

Even time steps

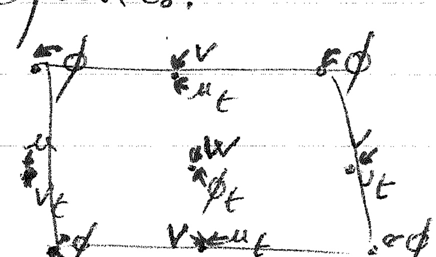

Odd time steps

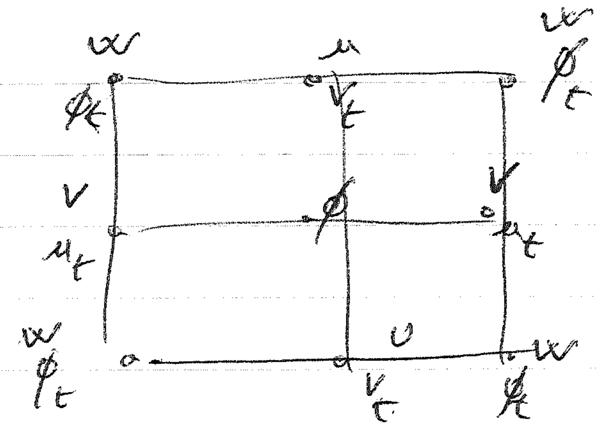

An analysis of this scheme can be found by Arakawa and Mesinger (1976)

8.2. Boundary conditions

They are important since they often define the problem. A first order ordinary differential equation such as $df/dx = 0$ specifies the solution as a constant. The boundary condition determines the value of this constant. A first order partial differential equation such as $\partial f(x,y)/\partial x = 0$ specifies very little of the solution. Any function $g(y)$ satisfies the equation and the boundary condition must specify $g(y)$.

The specification of computational boundary conditions, besides affecting numerical stability, greatly affects the accuracy of the finite difference solution.

a) Boundary conditions at the walls.

In addition to the no-normal ~~velocity~~ flux through the wall (normal velocity is zero), viscous boundary conditions are defined for the integration. The two most common are free-slip (the normal derivative of the velocity // to the wall is equal to zero $\Longleftrightarrow$ vorticity equal to zero on the boundary)

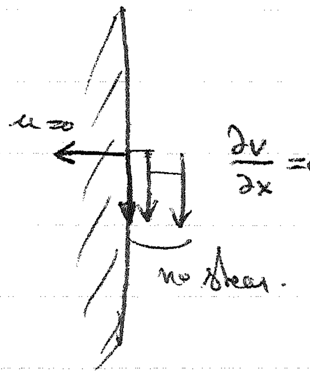

$\frac{\partial v}{\partial x} = 0 \Rightarrow \zeta_w = 0$ since u is constant on the wall

or no-slip (both u and v are equal to zero on the boundary, $\zeta_w \neq 0$)

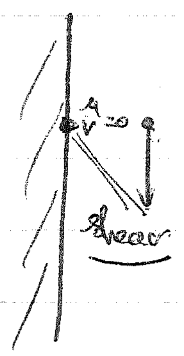

Implementation of this boundary condition varies depending on the mesh used.

Let's consider the vorticity equation and Poisson equation. We then need a boundary condition for the vorticity equation and one for the Poisson equation.

For free slip, in a regular mesh, $\zeta = 0$ and $\psi = 0$ are the needed BCs.

For no-slip, the streamfunction ψ can be expanded in Taylor series (vertical wall

$$(3) \quad \psi_{i+1,j} = \psi_{i,j} + \left.\frac{\partial \psi}{\partial x}\right|_{i,j} \Delta x + \frac{1}{2} \left.\frac{\partial^2 \psi}{\partial x^2}\right|_{i,j} \Delta x^2 + \cdots$$

The velocity $u = 0$ by the no-slip condition and

$$\left.\frac{\partial \psi}{\partial x}\right|_{i,j} = 0 \quad \text{and} \quad \left.\frac{\partial^2 \psi}{\partial x^2}\right|_{i,j} = \left.\frac{\partial v}{\partial x}\right|_{i,j}$$

$$\zeta = \frac{\partial v}{\partial x} - \frac{\partial u}{\partial y} \Longrightarrow \quad \frac{\partial u}{\partial y} = 0 \text{ because of } u = 0 \text{ and constant along the wall}$$

then $\zeta_w = \left.\dfrac{\partial v}{\partial x}\right|_{i,j}$

From (3), we derive the expression for the vorticity

$$\zeta_w = \frac{2(\psi_{i+1,j} - \overbrace{\psi_{i,j}}^{=0 \text{ at the wall.}})}{\Delta x^2}$$

One has to be careful about the possible over-specification of boundary conditions. For a no-slip wall, $u = v = 0$ and $\frac{\partial \psi}{\partial x} = \frac{\partial \psi}{\partial y} = 0$. Either of these condition is sufficient, but we cannot use both to solve the Poisson equation. On the other hand, $\psi = 0$ at the wall is sufficient, but is not to determine ζ_w. Therefore $\psi_w = 0$ is used for the Poisson equation and the $\frac{\partial \psi}{\partial x} = \frac{\partial \psi}{\partial y} = 0$ for the vorticity equation.

In staggered grid system, the expression for the vorticity might be different. Let's consider the case of the C-grid for a primitive equation model.

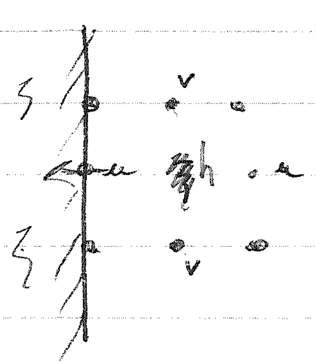

The u are defined on the wall, but not the v-velocities or the vorticity.

We therefore need to specify values of v "in" the boundary to recover the boundary condition

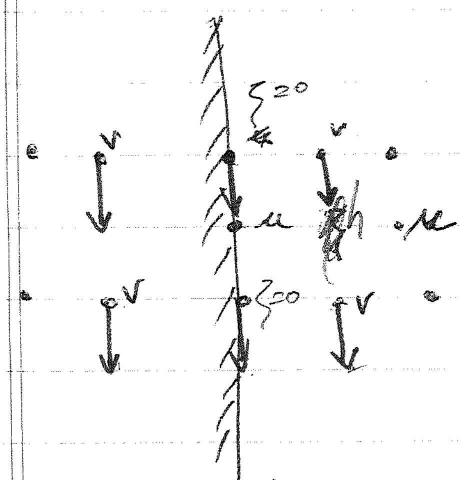

Free - Slip :

The v inside the wall have the same values as the one outside $\Rightarrow \zeta_w = 0$

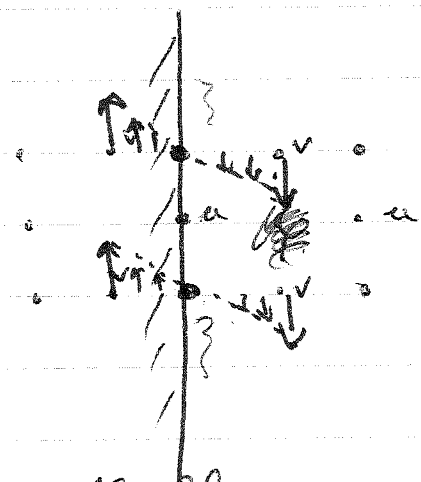

No - Slip :

The v inside the wall are opposite such that $v = 0$ at the wall

$$\zeta = \frac{2v}{\Delta x} = \frac{(v_{out} - v_{in})}{\Delta x}$$

b) upper - boundary (Rigid Lid approximation)

In the case of a primitive equation model, the time step must satisfy $\Delta t < \Delta x / c_{max}$ where c_{max} is the maximum phase speed that can occur in the system. These equations permit external and internal gravity waves inertial oscillations and Rossby waves. The external gravity waves have the speed $c \sim \sqrt{gH}$ which gives $c = 200\,m/s$ for $H = 4000\,m$ $\Longrightarrow$ very small Δt compared to the typical time scale of oceanic motions.

We can exclude the gravity waves by placing a lid at the surface or setting $w = 0$ at the upper boundary. A longer time step can be taken since the internal waves have a $c \lesssim 10\,m/s$.

<u>Basic equations</u>:

$$\begin{cases} \frac{d\vec{V}}{dt} = -\frac{1}{\rho_0}\vec{\nabla} p - f\vec{k}\times\vec{V} + \vec{F} & (4) \\ \frac{\partial p}{\partial z} = -\rho g & (5) \\ \frac{\partial w}{\partial z} + \nabla\cdot\vec{V} = 0 & (6) \end{cases}$$

Flat bottom + rigid lid give $w(0) = w(-H) = 0$
Integration of the continuity equation (6) gives

$$\boxed{\nabla\cdot\langle\vec{V}\rangle = 0} \qquad (7)$$

where $\langle(\ )\rangle = H^{-1}\int_{-H}^{0}(\ )\,dz$
The vertically averaged current is non divergent and a streamfunction can be introduced such that

$$\langle\vec{V}\rangle = \vec{k}\times\vec{\nabla}\psi \qquad (8)$$

We now take the vertical average of the equation of motion (4)

$$\frac{\partial}{\partial t}\langle\vec{V}\rangle = -\langle\vec{V}\cdot\nabla\vec{V} + w\frac{\partial V}{\partial z}\rangle \qquad (9)$$

$$-f\vec{k}\times\langle\vec{V}\rangle - \frac{1}{\rho_0}\vec{\nabla}\langle p\rangle + \langle\vec{F}\rangle$$

We can also form a vorticity equation
$(\vec{k}\cdot\nabla\times(9))$

$$\frac{\partial}{\partial t}\nabla^2\psi = -\vec{k}\cdot\vec{\nabla}\times\left(\langle\vec{V}\cdot\nabla\vec{V} + w\frac{\partial\vec{V}}{\partial z} + F\rangle\right.$$

$$-\langle V\rangle\cdot\nabla f \qquad (10)$$

This equation can be used to predict the mean vertical current ψ and $\langle V\rangle$

The departure from the mean is defined as

$$V = \langle V\rangle + V' \qquad (11)$$

Substituting in (4) and substracting (9), we obtain an equation for V'

(12) $$\frac{\partial \vec{V}'}{\partial t} = -\left(\vec{V}\cdot\nabla\vec{V} + w\frac{\partial \vec{V}}{\partial z}\right) + \langle \vec{V}\cdot\nabla\vec{V} + w\frac{\partial \vec{V}}{\partial z}\rangle - f\,\vec{k}\times\vec{V}' - \frac{1}{\rho_0}\vec{\nabla}p' + F - \langle F\rangle$$

where $p' = p - \langle p\rangle$

The hydrostatic equation (5) becomes

$$\frac{\partial p'}{\partial z} = -g\rho$$ which integrated from

$-H$ to z gives

(13) $$p' = p'(-H) - g\int_{-H}^{z}\rho\,dz$$

$\langle p'\rangle = 0 \Rightarrow$ (13) can be rewritten as

(14) $$p' = -g\int_{-H}^{z}\rho\,dz + g\langle\int_{-H}^{z}\rho\,dz\rangle$$

* First step, calculation of ψ using (10). This require a Poisson solver. ψ can be used to calculate $\langle\vec{V}\rangle$ from (8)

We then solve (12) for V' and the thermodynamic equation is advanced.

(15) $$\frac{d\theta}{dt} = A_\theta\nabla^2\theta + k_\theta\frac{\partial^2\theta}{\partial z^2} + \gamma_c(\theta)$$

and $$\rho = \rho_0\left[1 - \alpha\theta\right]$$, new density field

p' is then computed for use in (12).

Integration of the continuity equation gives the vertical velocity.

Another approach for large scale modelling other than the rigid lid is the use of ~~split~~-explicit time differencing scheme which treat the barotropic and baroclinic component of the flow with two different time step (small for barotropic, fast for baroclinic).
(9) (12)

This method treats the traveling ~~waves~~ Rossby waves more properly and in the case of irregular topography, avoids the use of a fast Poisson solver (problematic on non rectangular domains).

c) <u>Bottom topography</u>

Numerical techniques dealing with the modeling of topography in ocean and atmospheric models depend on the assumed vertical coordinate. They involve many difficulties regarding the model stability or the reliability of the results,

In z-coordinate, the most natural choice, each level dimension is independent of the bottom topography as well as of the horizontal location. The physical variables of the system are set equal to zero at the gridpoints located inside the bottom topography. The bottom topography is then represented by a succession of steps. Such a coordinate may be adapted for steep reliefs, but not for gentle slopes.

An alternative, extremely popular in the atmospheric models, is the σ-coordinate (or normalized pressure coordinate) after Phillips (1957) with $\sigma = p/p_s$ where p_s is the pressure at the bottom and is a function of x, y, t

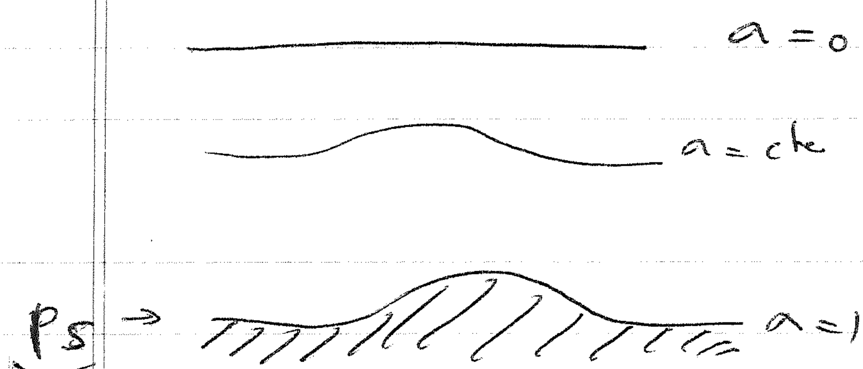

with $\frac{\partial \sigma}{\partial t} = 0$ on the surface

It conveniently avoids uncomfortable problems with the lowest boundary conditions. Nevertheless this coordinate also sets many problems, especially the non-cancellation of truncation errors (Smagorinsky et al., 1967). (See Haltiner and Williams for a review of the σ-coordinate system). Application to ocean models is fairly recent and preliminary conclusions are that σ-coordinates does pretty well with gentle slope (not steep) and vice-versa for z-coordinates.

The other coordinate which seems to handle all topographic situations well is the isopycnic system. Major problem is the intersection of the layers with the topography. This can be handled with a scheme which conserves the positiveness of the layer thickness such as FCT or Smolarkiewicz. Preliminary results from here (U of M) are extremely promising. (Bleck and Smith, 1990)

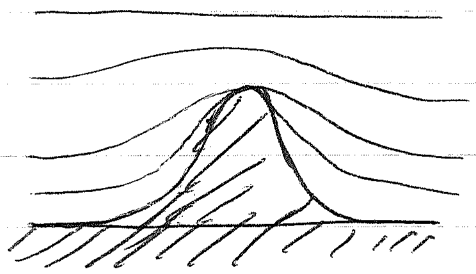

Steep topography in ocean models is under investigation (ARI, ONR).

d) <u>Irregular boundaries</u>

Irregular boundaries are everywhere in the ocean and do not facilitate the task of integrating the equations.

For example, in the case of a primitive equation model, introduction of a (x, y) bottom topography does not permit anymore to solve directly the Poisson equation (one direction vertical axis) and an iterative method such as the SOR (Successive Over-Relaxation technique) must be used or the split-explicit approach described in the previous section. The latter allows also for irregular lateral boundary conditions.

There is one method for either PE-flat bottom or QG which still allows for the use of a direct solver: the <u>Capacitance</u>

Matrix method (Carmus and Rysak, 1988, OPO adapted from Hockney, 1970)

The capacitance matrix method is a technique for extending the usefulness of direct solvers to non rectangular domains. The major computational burden of the method is that it requires to call twice the Poisson solver. It is in general more efficient than using an iterative method.

We wish to obtain a field which satisfies

(16) $$\nabla^2 \psi = \xi \qquad \psi, \xi \text{ function of } x, y$$

in a domain Ω with the condition $\psi = \psi_b$ on the boundary of $\Omega = d\Omega$

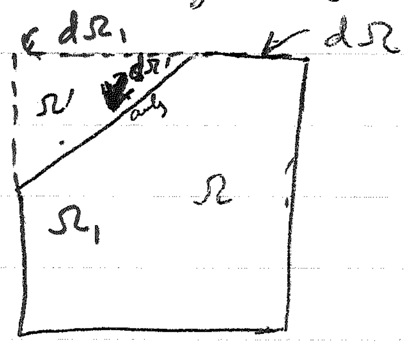

We can embed this domain into a rectangular one Ω_1. The difference is Ω' with $d\Omega_1$ and $d\Omega'$ their respective boundaries.

We first obtain through a direct solver the field ψ_1 in the Ω_1 domain by solving

(17) $$\nabla^2 \psi_1 = \xi_1 \qquad \text{where } \xi_1 = \xi \text{ in } \Omega$$

ξ_1 = arbitrary in Ω' and can be taken to be = to zero

Formally, the solution can be written as a function of the Green's functions associated with the operator ∇^2 such that

(18) $$\varphi_1 = \iint_{\Omega_1} G(x,y,x',y')\ \xi_1(x',y')\,dx'dy' + \int_{d\Omega_1} \varphi_1 \underbrace{\frac{\partial G}{\partial n}}_{\text{normal}} \, dl'_{\text{along}}$$

The Green's function G satisfies with δ = Dirac function.

(19) $$\begin{cases} \nabla^2 G = \delta(x-x')\,\delta(y-y') & \text{on } \Omega_1 \\ G = 0 & \text{on } d\Omega_1 \end{cases}$$

The essence of the capacitance matrix method is now to modify φ_1 such that $\varphi_1 = \varphi_b$ on $d\Omega'$. We then modify ξ_1 on $d\Omega'$ such that the solution satisfies the boundary condition.

We denoted $\theta(\vec{s})$, a function valid on on $\delta\Omega'$ only ($\vec{s}$, vector on the boundary $\delta\Omega'$). We consider the function $\mu(x,y)$ such that

(20) $$\nabla^2\mu = \xi_1 + \theta \quad \text{in } \Omega_1 \text{ with } \mu = \varphi_b \text{ on } \delta\Omega_1$$

If now $\theta(\vec{s})$ is chosen such that μ satisfies $\mu = \varphi_B$ on $\delta\Omega'$, then $\varphi(x,y) = \mu$ in Ω and the solution is found.

To determine $\theta(\vec{s})$, we use (18) and (19) to get the solution of (20)

(21) $$\mu(x,y) = \varphi_1 + \int_{d\Omega'} \theta(\vec{s})\ G(x,y,\vec{s})\, d\vec{s}$$

$\mu = \psi_b$ on $\delta\Omega'$ $\Rightarrow$ (21) reduces to

(22) $$\psi_b = \psi_1(\vec{s}) + \int_{\delta\Omega'} \theta(\vec{s}')\, G(x,y,\vec{s}')\, d\vec{s}'$$

which is an integral equation that determines $\theta(\vec{s})$

Application to finite - difference:

The curve $\delta\Omega'$ passes through a set of grid points referred to as the irregular boundary points.

1) The numerical algorithm first requires that we apply a direct solver to obtain ψ_1 in the rectangle given the forcing ζ_1

2) Next the modifying function θ is obtained from the values of ψ_1 along $\delta\Omega'$ by using (22) (discretized version).

3) The direct solver is employed a second time to solve (20) and to obtain ψ.

(22) is rewritten as $\psi_b = \psi_1 + \Delta s^2\, G\, .\, \theta$

where Δs = grid interval, θ, ψ_b, ψ_1 are column vectors of length m, (m = number of irregular boundary points)

The finite difference Green function, G, is a matrix $m \times m$.

(23) $$\theta = \Delta s^{-2}\, C\, (\psi_b - \psi_1)$$

where $C = G^{-1}$ = capacitance matrix

C has to be determined only once

G is determined from (19) by defining a delta function of strength Δ^{-2} and is placed at one irregular boundary. That satisfy for all the points.

Example

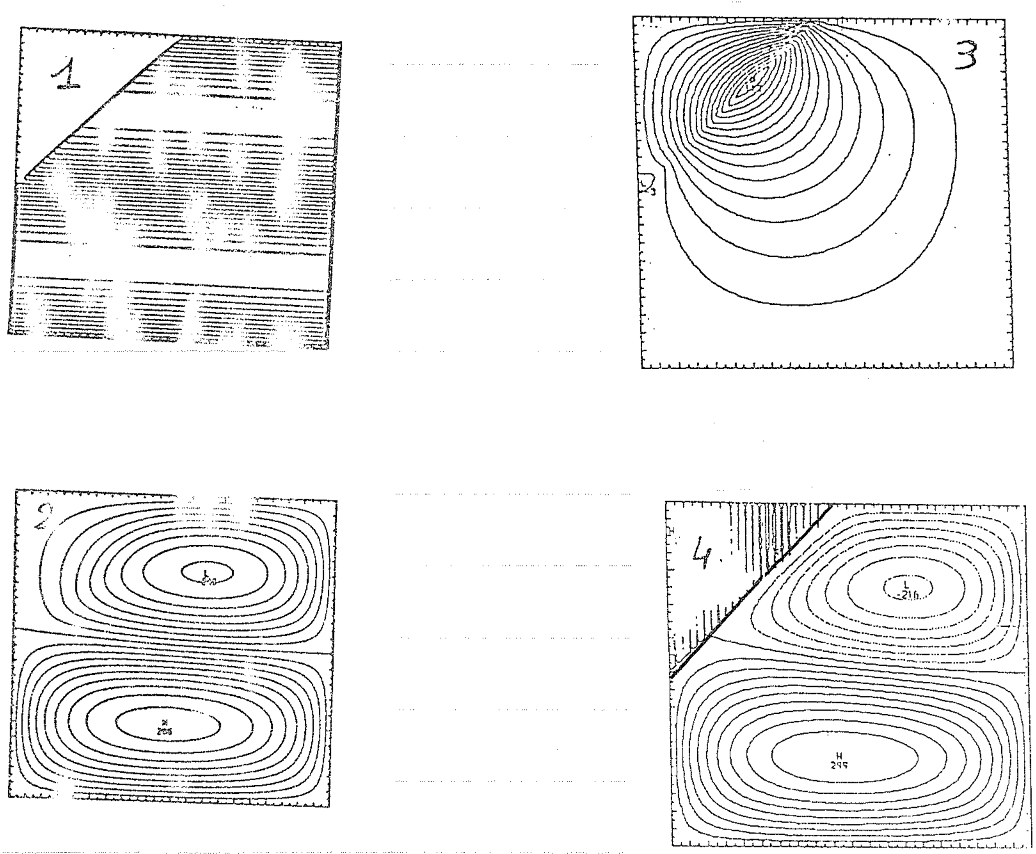

Original forcing field ζ_1

Corrective field Θ

ψ_1

Final ψ